Journal of Applied Physics ARTICLE pubs.aip.org/aip/jap

Auger and spin dynamics in a self-assembled quantum dot

Cite as: J. Appl. Phys. **134**, 154304 (2023); doi: 10.1063/5.0159775
Submitted: 26 May 2023 · Accepted: 27 September 2023 ·
Published Online: 19 October 2023

H. Mannel,[1,a)] J. Kerski,[1] P. Lochner,[1] M. Zöllner,[1] A. D. Wieck,[2] A. Ludwig,[2] A. Lorke,[1] and M. Geller[1]

AFFILIATIONS

[1]Faculty of Physics and CENIDE, University of Duisburg-Essen, 47057 Duisburg, Germany
[2]Lehrstuhl für Angewandte Festkörperphysik, Ruhr-Universität Bochum, 44780 Bochum, Germany

[a)]**Author to whom correspondence should be addressed:** hendrik.mannel@uni-due.de

ABSTRACT

The Zeeman-split spin states of a single quantum dot can be used together with its optical trion transitions to form a spin–photon interface between a stationary (the spin) and a flying (the photon) quantum bit. In addition to long coherence times of the spin state itself, the limiting decoherence mechanisms of the trion states are of central importance. Here, we investigate in time-resolved resonance fluorescence the electron spin and trion dynamics in a single self-assembled quantum dot in an applied magnetic field of up to $B = 10$ T. The quantum dot is only weakly coupled to an electron reservoir with tunneling rates of about $1\,\mathrm{ms}^{-1}$. Using this sample structure, we can measure, in addition to the spin-flip rate of the electron and the spin-flip Raman rate of the trion transition, the Auger recombination process that scatters an Auger electron into the conduction band. The Auger effect destroys the radiative trion transition and leaves the quantum dot empty until an electron tunnels from the reservoir into the dot. The combination of an Auger recombination event with subsequent electron tunneling from the reservoir can flip the electron spin and thus constitutes another mechanism that limits the spin lifetime.

I. INTRODUCTION

Self-assembled quantum dots (QDs)[1,2] are promising nanostructures that can host a single spin[3–6] to realize a quantum bit (qubit) in a solid-state environment.[7] The Zeeman-split states of the electron/hole spin in a magnetic field form here the two-level system for such a stationary qubit.[8] This spin qubit can be controlled via fast optical pulses[9,10] using the optically accessible trion states consisting of a pair of electrons in a spin-singlet state and an unpaired heavy-hole with spin-up or spin-down. However, to build a quantum computer,[7] or even more, a quantum Internet,[11,12] distant spins have to be transferred and entangled.[13–16] A prerequisite for this is that the coherent quantum state of the spin has to be mapped onto a flying qubit, a single photon[17] in a spin–photon interface.[18,19] Hence, long spin dephasing times for the stationary qubit and long coherence times for highly indistinguishable photons are needed for these envisioned quantum information technologies.

Single photons from (InGa)As self-assembled QDs have shown long coherence times,[20] high indistinguishability,[21,22] and long spin lifetimes.[23] However, a commonly neglected process has come more into the focus as it limits the coherence time of the spin and trion states: The Auger effect as an electron–electron scattering process, where the recombination energy of a trion is transferred to another excess electron/hole, that is ejected out of the QD into the conduction/valence band continuum. This scattering process is well known from colloidal QDs[24–26] and has been directly observed just recently in resonance fluorescence measurements[27] with Auger recombination rates in the order of microseconds.[28–31]

In this paper, we show time-resolved resonance fluorescence (RF) measurements on the trion transitions of a negatively charged InAs QD, embedded in an electrically controllable diode structure and charged by electron tunneling from a nearby charge reservoir. An applied magnetic field B of up to 10 T in Faraday geometry (here, parallel to the growth axis) splits the trion into a lower (red) and a higher (blue) energy transition. We address one of the trion transitions with a tunable diode laser and measure the decay of the fluorescence intensity in time. The observed transients involve the processes that quench the RF signal: The previously studied

spin-flip between the up- and down-spin states of the electron,[3,32,33] the spin-flip Raman scattering,[34] and, moreover, the Auger recombination. Using a rate equation model and a fit to the transients allows us to obtain the evolution of these scattering rates as a function of the applied magnetic field. The Auger rate shows a slight decrease as the magnetic field is switched on and stays constant within the accuracy of the measurement between 4 and 10 T. After an Auger recombination has emptied the QD, eventually an electron with opposite spin tunnels from the reservoir into the QD. This leads to an Auger-assisted spin dynamic which can limit the spin lifetime in a self-assembled QD for an optical spin read out via the trion transition. The Auger rate is important for an optical readout of the spin state because the Auger recombination empties the QD and resets the system to the ground state. This constitutes an efficient mechanism for spin randomization. A more detailed understanding of the Auger effect with its dependence on a magnetic field will help decrease the Auger recombination and enhance the spin-lifetime in future optimized QD structures.

II. SAMPLE DESIGN AND METHODS

The measurements were performed on a single self-assembled (InGa)As QD at 4.2 K in a confocal microscope setup. The sample contains a single layer of QDs and was grown by molecular beam epitaxy.[2] During the growth process, the QDs were In-flushed[35] to shift the emission wavelength to ≈950 nm. The QD layer is embedded in a p–i–n diode structure with a highly n-doped GaAs layer as a charge reservoir and a highly p-doped GaAs layer as an epitaxial gate.[36] Between the charge reservoir and the QD, 45 nm (AlGa)As are implemented as tunneling barrier to achieve electron tunneling times in the order of milliseconds (see Lochner *et al.*[30] for details about the sample structure). An applied voltage between charge reservoir and gate can control the charge state of the QD.[28,37] Furthermore, the resonance of the QD can be tuned by the quantum confined Stark effect.[38] The QD is optically investigated by resonance fluorescence, where the laser background is suppressed by cross polarization.[39]

III. QUANTUM DOT STATES AND TRANSITIONS IN A MAGNETIC FIELD

In Fig. 1(a), the RF signal of the negatively charged exciton, the so-called trion (X^-), is shown as a function of gate voltage and laser frequency. In the gate voltage range from 0.38–0.58 V (area B), the QD is charged with one electron, and RF from the trion can be observed. At lower gate voltages (area A), the QD is empty, while at higher voltages (area C), it is charged with two electrons (see also Lochner *et al.*[40]). In both cases, the trion transition is forbidden. When a magnetic field (Faraday geometry) is applied to the sample, the trion state will not be spin-degenerated anymore and will split up into an energetically lower ("red trion" with spin configuration $|\uparrow\downarrow\Downarrow\rangle$) and an energetically higher state ("blue trion" with spin configuration $|\uparrow\downarrow\Uparrow\rangle$).[3] For the specific QD investigated here, this can be seen in Fig. 1(b). In this measurement, a gate voltage of 0.5 V is applied, and the laser frequency is tuned to match the blue and red trion resonance. The energy difference between the two trion resonances increases linearly due to the Zeeman effect,[41] while their mean value follow a diamagnetic shift.

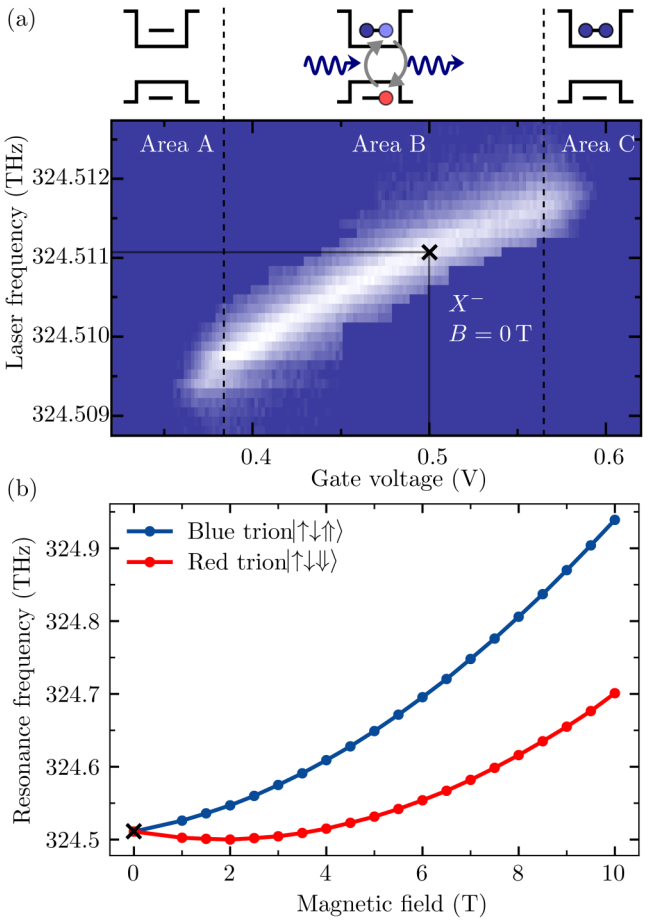

FIG. 1. (a) RF intensity of the trion transition as a function of gate voltage and laser frequency. In the interval from $V_G = 0.38$ to 0.58 V (area B), the QD is charged with one electron and the trion transition is observed at laser frequencies between 324.5095 and 324.5115 THz. In area A, the QD is empty. In area C, it is charged with two electrons. (b) Magnetic field dependence of the trion resonance frequencies at $V_G = 0.5$ V. The data point at $B = 0$ is taken from (a) (black cross). At $B \neq 0$, the trion transition splits into an energetically lower (red) and an energetically higher (blue) transition.

IV. MODEL

Figure 2 schematically shows the energy diagram in a magnetic field with the spin-up $|\uparrow\rangle$ and spin-down $|\downarrow\rangle$ ground states that form, together with the transitions to the red ($|\uparrow\downarrow\Downarrow\rangle$) and blue trion ($|\uparrow\downarrow\Uparrow\rangle$), two Lambda-schemes.[34,42–44] Here, we add the crystal ground state $|0\rangle$ to the Lambda-schemes in Fig. 2 as this state is accessible by the Auger recombination process (see discussion below). In a magnetic field, we resonantly excite the blue transition by a laser field with Rabi frequency Ω_R to the trion configuration $|\uparrow\downarrow\Uparrow\rangle$, which is an electron singlet state with an additional heavy-hole with spin projection $m_z = 3/2$ (see Fig. 2). An optical transition with the spontaneous emission rate Γ emits a photon, and the spin-up ground state $|\uparrow\rangle$ is recovered. In addition,

but with much smaller probability (branching rations Γ/γ_R of 10^3 above $B = 60\,\mathrm{mT}$[34]), a spin-flip Raman process[45] is possible. In addition, at large magnetic fields, relaxation via the red trion $|\uparrow\downarrow\Uparrow\rangle$ is possible due to mixing between the heavy and the light holes. This process has the same effect in this measurement and is, therefore, part of the rate γ_R. Because of the energy mismatch between the "blue" laser excitation and the "red" trion transition, the RF signal is switched off until a spin relaxation into the initial spin-up state $|\uparrow\rangle$ with rate κ_2 has occurred. The spin-flip is mediated by spin–orbit coupling[33] or hyperfine interaction to the nuclei-spin bath.[46–48] It is also possible that a spin-flip in the QD occurs in the opposite direction from $|\uparrow\rangle$ to $|\downarrow\rangle$ with the rate κ_1. The ratio of κ_1 and κ_2 will be discussed later. As long as the QD is in the $|\downarrow\rangle$ state, no blue trion transition is possible. Thus, both, the spin-flip Raman process and the direct spin-flip from the $|\uparrow\rangle$-state to the $|\downarrow\rangle$-state, reduce the RF signal by scattering into the dark spin-down $|\downarrow\rangle$ state. For $B = 0\,\mathrm{T}$, both spin states are degenerated as both trion states. Furthermore, we excite with strictly linearly polarized light (measured extinction ratio $> 10^8:1$). Therefore, both spin states are indistinguishable in our experiment and the level scheme in Fig. 2 reduces to a three state system with only one remaining fit parameter γ_A (see the supplementary material).

Another important effect, which can switch off the RF of the blue trion transition, is the Auger effect (arrow from $|\downarrow\uparrow\Uparrow\rangle$ to $|0\rangle$ in Fig. 2). In this non-radiative process, the recombination energy of an electron–hole pair is transferred to the additional electron in the dot, which subsequently is emitted with rate γ_A into the conduction band. Hence, the QD is in the crystal ground state $|0\rangle$. The Auger-mediated electron emission is proportional to the Auger rate

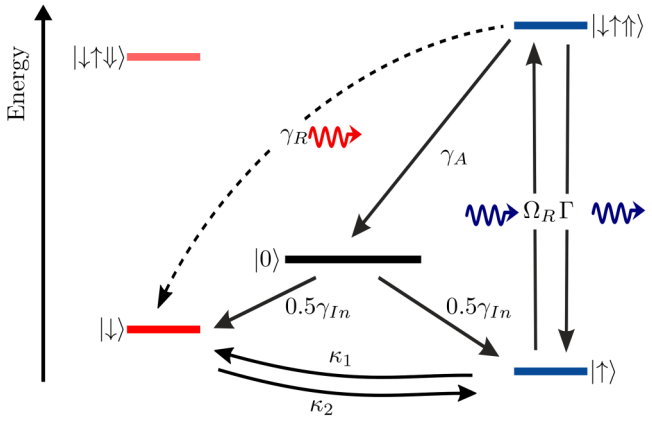

FIG. 2. Level scheme of the singly charged QD in a magnetic field (Faraday geometry) with transitions. The spin states $|\downarrow\rangle$ and $|\uparrow\rangle$ are energetically splitted by the Zeeman effect. The optical transition to the energetically higher blue trion state $|\uparrow\downarrow\Uparrow\rangle$ is excited with the Rabi frequency Ω_R and decays spontaneously with rate Γ. The trion state can also decay via a spin-flip Raman process with the rate γ_R into the spin state $|\downarrow\rangle$ or via a non-radiative Auger recombination with the rate γ_A into the crystal ground state $|0\rangle$. By tunneling of an electron with random spin orientation, states $|\downarrow\rangle$ and $|\uparrow\rangle$ get occupied. The electron spin can flip from $|\downarrow\rangle$ to $|\uparrow\rangle$ with the spin relaxation rate κ_2 and inversely with rate κ_1.

γ_A and the average occupation of the QD with a trion n, see Eq. (1).[30,31] The Auger recombination is often neglected, especially in samples with small tunneling barriers and tunneling rates faster than the spontaneous emission lifetime, which is in the order of $\Gamma \approx 1\,\mathrm{ns}^{-1}$.[49] In these samples with strong tunnel-coupling, the Auger-emitted electron is replaced immediately by tunneling from the charge reservoir. However, the Auger effect still decreases the emitted intensity and empties the QD. The empty QD can be recharged with an electron by tunneling from the reservoir with rate γ_{In} either into the spin-up $|\uparrow\rangle$ or the spin-down state $|\downarrow\rangle$. From a dark spin-down state $|\downarrow\rangle$, the QD can be reset to the bright spin-up state $|\uparrow\rangle$ by a spin-flip with rate κ_2. A spin-flip in the opposite direction is also possible with the rate κ_1.[34] In summary, as the blue trion can only be excited from state $|\uparrow\rangle$, there are three processes, which decrease the RF signal: (i) a direct spin-flip from the spin-up to the spin-down state with rate κ_1, (ii) a spin-flip Raman process with rate γ_R, and (iii) an Auger recombination with rate γ_A. For process (i) and (ii), a subsequent spin-flip with rate κ_2 is required to return to the optical bright state $|\uparrow\rangle$. The Auger process for case (iii) needs electron tunneling from the charge reservoir with rate γ_{In} and, if the QD is recharged with a spin-down electron, an additional spin-flip to get to the bright spin-up state $|\uparrow\rangle$ again.

V. MEASUREMENTS

To investigate the described Auger and spin dynamics of charge carriers in a single self-assembled QD in a magnetic field, we use time-resolved RF. The measurement scheme can be seen in Fig. 3(a), where the laser intensity, the gate voltage, and the expected RF signal are displayed. A single shot consists of three parts: (1) the preparation, (2) the probing of the QD, and (3) the background correction of the signal. In (1), the QD is prepared in the ground state. That means, one electron is charged in the QD, hence, it is either in state $|\uparrow\rangle$ or in state $|\downarrow\rangle$. To achieve this, the laser is turned off and the gate voltage is set to 0.5 V [which is in area B in Fig. 1(a)] for 2 ms, which is longer than the tunneling time $t_{In} = 1/\gamma_{In}$ plus the time until a thermal equilibrium between states $|\uparrow\rangle$ and $|\downarrow\rangle$ is reached. At a gate voltage of 0.5 V, the Fermi distribution in the reservoir is unity and the tunneling rate out of the dot is nearly zero and, therefore, neglected. This was measured in a similar sample structure in Kurzmann *et al.* (see Figs. 2 and 3).[50] This is also the reason for the ability to charge the QD deterministically.

The occupation probability of these states in thermal equilibrium at the end of the preparation step (1) has a minor effect on the determination of the involved rates; however, it can be easily estimated: In equilibrium, the occupation of both states follow a Boltzmann distribution at 4.2 K[34] with the energy splitting of the spin-up state $|\uparrow\rangle$ and the spin-down state $|\downarrow\rangle$. The energy of the spin-splitting is approximated by using the energy splitting of the red and blue trion resonance as shown in Fig. 1(b). With an electron g-factor at our transition energy of 1.33 eV of about $g_e = 0.8$[45] and an hole g-factor of $g_h = 0.2$, the hole is neglected here as a reasonable approximation. As an example, for a magnetic field of 4 T, this results in thermal occupation probabilities of about 65% for the spin-up state $|\uparrow\rangle$ and 35% for the spin-down state $|\downarrow\rangle$.

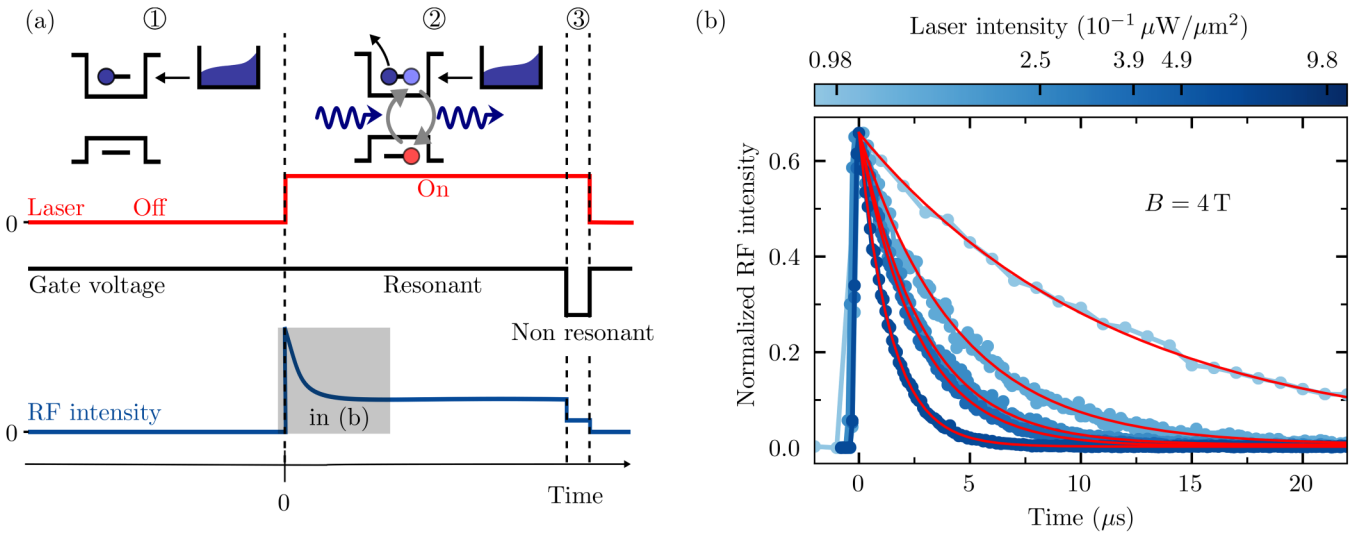

FIG. 3. Time-resolved RF n-shot measurement of the Auger effect and spin dynamics in a magnetic field. (a) One shot consists of the preparation (1) and probing (2) of the QD and the background correction of the signal (3). (1) The QD is prepared with one electron by switching off the laser (red line) and setting $V_G = 0.5$ V (black line). (2) The laser (resonant with the blue trion transition) is switched on, and V_G remains at 0.5 V. As the QD is prepared with one electron, the expected RF signal (blue line) will switch on and decrease afterward due to Auger recombination and the spin-flip Raman process. (3) To account for spurious signals (dark counts and reflected laser light), the gate voltage is shortly detuned to −0.5 V, where the QD is off resonance. This background is subtracted from the measured RF signal. (b) Normalized RF intensity in area (2) for a magnetic field of 4 T. While the laser is turned on and the QD is in resonance, decreasing transients are observed. The measured transients (blue) along with fits by the rate model (red lines) are shown for different laser intensities.

The difference between the occupation probabilities increases up to an occupation probability of 93% for $|\uparrow\rangle$ and 7% for $|\downarrow\rangle$ at $B = 10$ T. The ratio of occupation probabilities of states $|\uparrow\rangle$ and $|\downarrow\rangle$ will also be used to describe the ratio of the spin-flip rates κ_2 and κ_1.

In step (2) in Fig. 3(a), at $t = 0$, the laser is switched on and excites resonantly the blue trion transition while the RF signal is recorded. As the excited blue trion can also decay via Auger recombination or the spin-flip Raman process, the QD can end up either in the crystal ground state $|0\rangle$ or the spin-down state $|\downarrow\rangle$ (see Fig. 2); no RF signal can be recorded until an electron tunnels into the dot or a spin-flip has occurred. In an n-shot time-resolved measurement, a decreasing transient of the RF intensity is observed, starting with a maximum at $t = 0$ [see blue line in Fig. 3(a)] and a saturation behavior for $t \gg 0$ until dynamic equilibrium is reached. The trion transition is turned "off" in equilibrium by electron emission via Auger recombination or spin-flip Raman scattering and "on" again by electron tunneling or a spin-flip process (see Fig. 2). At step (3) in the time sequence, the gate voltage is switched to −0.5 V [area A in Fig. 1(a)] to measure the laser background and APD dark counts for background correction. For a good signal to noise ratio, 50 000 to 100 000 transient shots were accumulated. This also averages out fluctuations of the trion occupation n due to laser intensity fluctuations or noise in the sample.

These time-resolved n-shot RF measurements are performed for magnetic fields of 0, 4, 6, 8, and 10 T. For each magnetic field, the time-resolved RF signal is recorded at different laser excitation intensities ranging from 9.8×10^{-2} up to $9.8 \times 10^{-1}\,\mu$W/μm^2. As expected, the RF signal shows decreasing transients starting from $t = 0$. As an example, the measured transients at a magnetic field of 4 T can be seen in Fig. 3(b) (blue) for different laser intensities. The measured background is subtracted for each transient, and they are normalized to the ground-state occupation probability of the spin-up state $|\uparrow\rangle$, which is 65% at 4 T (see discussion above). With increasing laser intensity, the RF intensity decreases faster. For all shown laser intensities, the transients saturate after >0.06 ms.

VI. RESULTS AND DISCUSSION

The fluorescent optical transition between the spin-up $|\uparrow\rangle$ ground state and the excited trion state $|\uparrow\downarrow\Uparrow\rangle$ (resonant excitation and spontaneous emission) are orders of magnitude faster than the Auger, spin-flip and spin-flip Raman scattering. Therefore, we combine the spin-up and the trion state into one state $|1\rangle$ and distinguish now between three different states:[31] Two non-fluorescent (optically dark) states $|0\rangle$ (after an Auger process) and $|\downarrow\rangle$ (after a spin-flip Raman process) and one fluorescent (optically bright) state $|1\rangle$. Three rate equations for these three states with the parameters for the transition rates and the average occupation in the trion state n (see supplementary material) describe the dynamics of the quantum system as shown in Fig. 2,

$$\dot{P}_{|0\rangle}(t) = n \cdot \gamma_A \cdot P_{|1\rangle}(t) - \gamma_{In} \cdot P_{|0\rangle}(t), \quad (1)$$

$$\dot{P}_{|\downarrow\rangle}(t) = 0.5 \cdot \gamma_{In} \cdot P_{|0\rangle}(t) + (1-n) \cdot \kappa_1 \cdot P_{|\uparrow\rangle}(t) + n \cdot \gamma_R \cdot P_{|\uparrow\rangle}(t) - \kappa_2 \cdot P_{|\downarrow\rangle}(t), \quad (2)$$

$$\dot{P}_{|\uparrow\rangle}(t) = 0.5 \cdot \gamma_{In} \cdot P_{|0\rangle}(t) + \kappa_2 \cdot P_{|\downarrow\rangle}(t) - (1-n) \cdot \kappa_1 \cdot P_{|\uparrow\rangle}(t) - n \cdot (\gamma_A + \gamma_R) \cdot P_{|\uparrow\rangle}(t). \quad (3)$$

The sum of all probabilities $P_{|0\rangle}$, $P_{|\downarrow\rangle}$, and $P_{|\uparrow\rangle}$ must be 1 for every time t. The initial conditions at $t = 0$, as well as the ratio of κ_1 and κ_2, are given by the earlier described Boltzmann distribution for each magnetic field. At $B = 4$ T, the conditions are $P_{|0\rangle}(0) = 0$, $P_{|\downarrow\rangle}(0) = 0.35$, and $P_{|\uparrow\rangle}(0) = 0.65$. The measured RF intensity is proportional to the rate of photons emitted from the radiative trion recombination. The tunneling rate into the dot γ_{In} is determined for every magnetic field in a separate measurement (see the supplementary material). $\dot{P}_{|\uparrow\rangle}(t)$ describes the temporal development of the normalized RF intensity and is numerically integrated with the remaining three free parameters: the Auger rate γ_A, the spin-flip rate from state $|\downarrow\rangle$ to state $|\uparrow\rangle$ κ_1, and the spin-flip Raman rate γ_R. $\dot{P}_{|\uparrow\rangle}(t)$ is used to fit the measured data for every excitation laser intensity in each magnetic field. For 4 T, the fits are shown as red lines in Fig. 3(b) in good agreement with the blue data points. From these fits, we have determined the values of the Auger, spin-flip Raman, and spin relaxation rates in Fig. 4. The blue lines in Fig. 4 show the rates for increasing laser intensity from 0.098 up to 0.98 μW/μm^2. As expected, the Auger rate γ_A and the spin-flip Raman rate γ_R are within the accuracy of the measurement, independent of the laser excitation intensity. The Auger rate γ_A and the spin-flip Raman rate γ_R are directly obtained by including the average occupation with a trion n into our rate equation model. Thus, we will concentrate on the average rates, shown as red lines in Fig. 4. We have checked the quality for three fitting parameters by fixing different rates at different values (see the supplementary material for more information). Also, we have compared the spin-flip rate κ_2 and the spin-flip Raman rate γ_R with values from the literature, discussed in the following.

The spin-flip rate, shown in Fig. 4(c), has been measured before, for instance, by Kroutvar *et al.*[33] and Lu *et al.*,[32] and gives, hence, a good checkpoint for our fitting routines for the unknown Auger and spin-flip Raman rate. We observe a spin-flip rate of $\kappa_2 = 1.58\,\text{ms}^{-1}$ at $B = 4$ T, increasing up to $34.8\,\text{ms}^{-1}$ at $B = 10$ T, having a power-law dependence with an exponent of $m = 3.4$ (see the supplementary material). These values and the dependence of the spin-flip rates are in good agreement with those from the literature. The spin-flip Raman rate [Fig. 4(b)] is constant in the magnetic field. Spin-flip Raman scattering is mainly due to two effects: at low magnetic fields, the hyperfine interaction with the nuclear spins leads to an effective magnetic field (Overhauser field), where the transverse component mixes both spin-up and spin-down states. In high magnetic fields, the mixing of the light- and heavy holes[8,34] and the small contribution of the light hole state makes a transition into the opposite spin state possible. We show here that, up to 10 T, the spin-flip Raman scattering rate γ_R is always more than two order of magnitude faster than the spin-flip rate.

This observation is in good agreement with the opportunity to use the spin-flip Raman scattering process for spin-pumping[32] since the Raman process scatters faster into the spin-down state $|\downarrow\rangle$ than the spin-flip can scatter back into the spin-up state $|\uparrow\rangle$. This is even more effective at smaller magnetic fields, where the ratio γ_R/κ_2 exceeds a factor of 10^3. This ratio also explains the lack of data between 0 and 4 T. The spin-up electron can be pumped into the dark state (here $|\downarrow\rangle$) via a spin-flip Raman process, while at the same time the spin-flip rate κ_2 is very small in low magnetic fields [see Fig. 4(c)]. As a consequence, it takes a long time to return into the resonantly excited blue trion state, and the RF signal is too small to be measured. At higher magnetic fields, the spin-flip rate is fast enough to recover the RF of the blue trion.

Finally, Fig. 4(a) shows the Auger rate γ_A at $B = 0$ and $B = 4$–10 T. At $B = 0$, the Auger rate is around $3\,\mu\text{s}^{-1}$ for all laser excitation intensities; in agreement with previous measurements on almost identical InAs/GaAs QDs.[30,31] At $B = 4$ T, the Auger rate

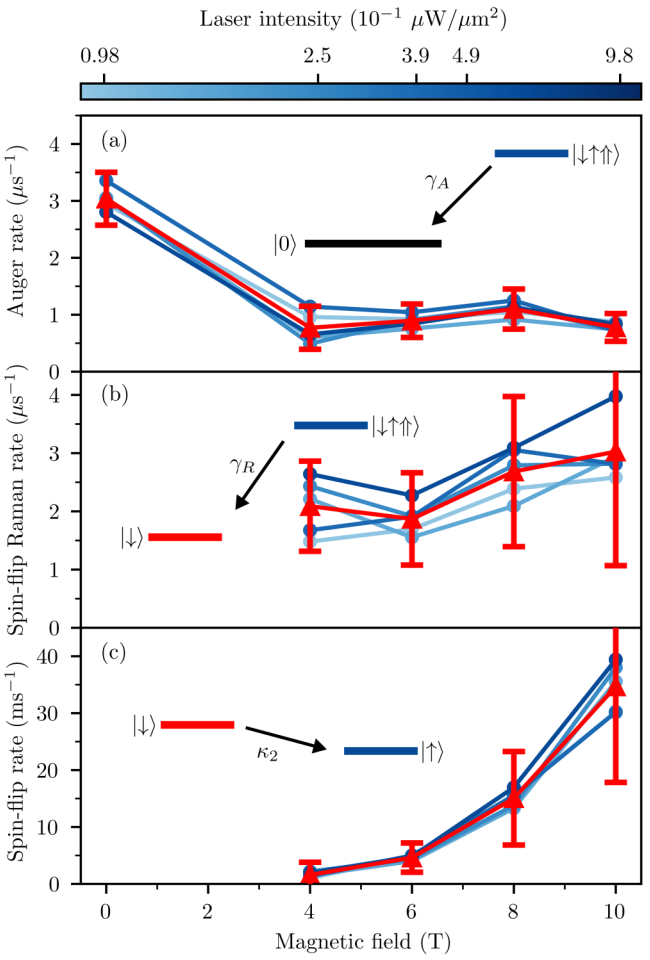

FIG. 4. Magnetic field dependence of the Auger rate (a), spin-flip Raman rate (b), and spin-flip rate (c) for different laser intensities (blue shades, circles), obtained from fits of the numerical solution of Eq. (2). The average rates over all laser intensities for each magnetic field are shown in red triangles. At 0 T, the trion transition degenerates, and we are unable to extract spin-flip nor spin-flip Raman processes with our method.

has dropped below $1\,\mu s^{-1}$ and remains, within the accuracy of the measurement, almost constant up to $B = 10$ T. This is in contrast to a naïve expectation of a increasing Auger rate with increasing magnetic field. Indeed, additional magnetic confinement is evidenced by the diamagnetic shift [see Fig. 1(b)]. This stronger carrier confinement implies a larger carrier overlap and thus should increase the Auger rate. We observe the opposite, so our finding needs another explanation. Further experimental studies and theoretical calculations including the final density of states for the Auger-scattered electron in the conduction band will shed light to our observation.

VII. CONCLUSION

In conclusion, we have presented time-resolved resonance fluorescence measurements on the blue trion transition of a self-assembled QD in an applied magnetic field. The resonant pumping of the trion transition and the decay of the fluorescence intensity allows to study the underlying processes, where in a weakly tunnel-coupled dot (tunneling rates of about 1/ms) not only the spin-flip and spin-flip Raman processes but the Auger recombination can be observed. The spin-flip rate increases for increasing magnetic field. The spin-flip Raman rate γ_R stays constant in the magnetic field, while the Auger rate shows a drop by a factor of three in a magnetic field. The combination of an Auger recombination and electron tunneling event has a 50% chance to flip the electron spin. The Auger rate is several orders of magnitude larger than the spin-flip rate. Thus, it can significantly limit the spin lifetime in quantum-dot-based devices for quantum information technologies, while longer spin lifetimes are desired. In addition to adapting the QD shape and size, our study points toward an additional tuning knob: A superlattice around the quantum dot in the device structure could form sub-bands with bandgaps to suppress the Auger effect by reducing the final density of state for the Auger electron.

SUPPLEMENTARY MATERIAL

The supplementary material consists of additional measurements that are mentioned in the text.

ACKNOWLEDGMENTS

This work was funded by the Deutsche Forschungsgemeinschaft (DFG, German Research Foundation)—Project-ID 278162697–SFB 1242 and the individual Research Grant No. GE2141/5-1. A.Lu. acknowledge gratefully the support of the DFG by Project No. LU2051/1-1. A.Lu. and A.D.W. acknowledges support by Grant Nos. DFG-TRR160, BMBF-QR.X KIS6QK4001, and DFH/UFA CDFA-05-06.

AUTHOR DECLARATIONS

Conflict of Interest

The authors have no conflicts to disclose.

Author Contributions

H. Mannel: Data curation (lead); Formal analysis (lead); Investigation (lead); Validation (equal); Visualization (equal); Writing – original draft (lead); Writing – review & editing (equal). **J. Kerski:** Formal analysis (equal); Supervision (equal); Validation (equal); Writing – review & editing (equal). **P. Lochner:** Formal analysis (equal); Supervision (equal); Validation (equal); Writing – original draft (equal); Writing – review & editing (equal). **M. Zöllner:** Data curation (equal); Formal analysis (equal); Visualization (supporting); Writing – review & editing (equal). **A. D. Wieck:** Project administration (supporting); Resources (supporting); Writing – review & editing (supporting). **A. Ludwig:** Project administration (supporting); Resources (equal); Writing – review & editing (supporting). **A. Lorke:** Conceptualization (equal); Formal analysis (supporting); Funding acquisition (equal); Project administration (equal); Resources (equal); Supervision (equal); Visualization (supporting); Writing – review & editing (supporting). **M. Geller:** Conceptualization (lead); Data curation (supporting); Formal analysis (supporting); Funding acquisition (equal); Investigation (equal); Project administration (equal); Supervision (equal); Validation (equal); Visualization (equal); Writing – original draft (supporting); Writing – review & editing (equal).

DATA AVAILABILITY

The data that support the findings of this study are available from the corresponding author upon reasonable request.

REFERENCES

[1]D. Bimberg, M. Grundmann, and N. Ledentsov, *Quantum Dot Heterostructures* (John Wiley & Sons, 1999).
[2]P. M. Petroff, A. Lorke, and A. Imamoglu, "Epitaxially self-assembled quantum dots," Phys. Today **54**(5), 46–52 (2001).
[3]M. Atature, "Quantum-dot spin-state preparation with near-unity fidelity," Science **312**, 551–553 (2006).
[4]A. Imamoglu, D. D. Awschalom, G. Burkard, D. P. DiVincenzo, D. Loss, M. Sherwin, and A. Small, "Quantum information processing using quantum dot spins and cavity QED," Phys. Rev. Lett. **83**, 4204–4207 (1999).
[5]R. Hanson and D. D. Awschalom, "Coherent manipulation of single spins in semiconductors," Nature **453**, 1043–1049 (2008).
[6]S. Benjamin, B. Lovett, and J. Smith, "Prospects for measurement-based quantum computing with solid state spins," Laser Photonics Rev. **3**, 556–574 (2009).
[7]T. D. Ladd, F. Jelezko, R. Laflamme, Y. Nakamura, C. Monroe, and J. L. O'Brien, "Quantum computers," Nature **464**, 45–53 (2010).
[8]T. Calarco, A. Datta, P. Fedichev, E. Pazy, and P. Zoller, "Spin-based all-optical quantum computation with quantum dots: Understanding and suppressing decoherence," Phys. Rev. A **68**, 012310 (2003).
[9]D. Press, T. D. Ladd, B. Zhang, and Y. Yamamoto, "Complete quantum control of a single quantum dot spin using ultrafast optical pulses," Nature **456**, 218–221 (2008).
[10]B. D. Gerardot, D. Brunner, P. A. Dalgarno, P. Öhberg, S. Seidl, M. Kroner, K. Karrai, N. G. Stoltz, P. M. Petroff, and R. J. Warburton, "Optical pumping of a single hole spin in a quantum dot," Nature **451**, 441–444 (2008).
[11]B. D. Lio, C. Faurby, X. Zhou, M. L. Chan, R. Uppu, H. Thyrrestrup, S. Scholz, A. D. Wieck, A. Ludwig, P. Lodahl, and L. Midolo, "A pure and indistinguishable single-photon source at telecommunication wavelength," Adv. Quantum Technol. **5**, 2200006 (2022).
[12]H. J. Kimble, "The quantum internet," Nature **453**, 1023–1030 (2008).
[13]M. L. Chan, A. Tiranov, M. H. Appel, Y. Wang, L. Midolo, S. Scholz, A. D. Wieck, A. Ludwig, A. S. Sørensen, and P. Lodahl, "On-chip spin-photon entanglement based on single-photon scattering," NPJ Quant. Info. **1**, 9 (2023).

[14]A. Delteil, Z. Sun, W. Gao, E. Togan, S. Faelt, and A. Imamoğlu, "Generation of heralded entanglement between distant hole spins," Nat. Phys. **12**, 218–223 (2016).
[15]H. Bernien, B. Hensen, W. Pfaff, G. Koolstra, M. S. Blok, L. Robledo, T. H. Taminiau, M. Markham, D. J. Twitchen, L. Childress, and R. Hanson, "Heralded entanglement between solid-state qubits separated by three metres," Nature **497**, 86–90 (2013).
[16]B. Hensen, H. Bernien, A. E. Dréau, A. Reiserer, N. Kalb, M. S. Blok, J. Ruitenberg, R. F. L. Vermeulen, R. N. Schouten, C. Abellán, W. Amaya, V. Pruneri, M. W. Mitchell, M. Markham, D. J. Twitchen, D. Elkouss, S. Wehner, T. H. Taminiau, and R. Hanson, "Loophole-free Bell inequality violation using electron spins separated by 1.3 kilometres," Nature **526**, 682–686 (2015).
[17]M. Atatüre, D. Englund, N. Vamivakas, S.-Y. Lee, and J. Wrachtrup, "Material platforms for spin-based photonic quantum technologies," Nat. Rev. Mater. **3**, 38–51 (2018).
[18]A. Javadi, D. Ding, M. H. Appel, S. Mahmoodian, M. C. Löbl, I. Söllner, R. Schott, C. Papon, T. Pregnolato, S. Stobbe, L. Midolo, T. Schröder, A. D. Wieck, A. Ludwig, R. J. Warburton, and P. Lodahl, "Spin–photon interface and spin-controlled photon switching in a nanobeam waveguide," Nat. Nanotechnol. **13**, 398–403 (2018).
[19]W. B. Gao, P. Fallahi, E. Togan, J. Miguel-Sanchez, and A. Imamoglu, "Observation of entanglement between a quantum dot spin and a single photon," Nature **491**, 426–430 (2012).
[20]C. Matthiesen, A. N. Vamivakas, and M. Atatüre, "Subnatural linewidth single photons from a quantum dot," Phys. Rev. Lett. **108**, 093602 (2012).
[21]C. Matthiesen, M. Geller, C. H. H. Schulte, C. L. Gall, J. Hansom, Z. Li, M. Hugues, E. Clarke, and M. Atatüre, "Phase-locked indistinguishable photons with synthesized waveforms from a solid-state source," Nat. Commun. **4**, 1600 (2013).
[22]C. Santori, D. Fattal, J. Vučković, G. S. Solomon, and Y. Yamamoto, "Indistinguishable photons from a single-photon device," Nature **419**, 594–597 (2002).
[23]G. Gillard, I. M. Griffiths, G. Ragunathan, A. Ulhaq, C. McEwan, E. Clarke, and E. A. Chekhovich, "Fundamental limits of electron and nuclear spin qubit lifetimes in an isolated self-assembled quantum dot," npj Quantum Inf. **7**, 43 (2021).
[24]R. Vaxenburg, A. Rodina, A. Shabaev, E. Lifshitz, and A. L. Efros, "Nonradiative Auger recombination in semiconductor nanocrystals," Nano Lett. **15**, 2092–2098 (2015).
[25]A. W. Cohn, J. D. Rinehart, A. M. Schimpf, A. L. Weaver, and D. R. Gamelin, "Size dependence of negative trion Auger recombination in photodoped CdSe nanocrystals," Nano Lett. **14**, 353–358 (2014).
[26]A. L. Efros and M. Rosen, "Random telegraph signal in the photoluminescence intensity of a single quantum dot," Phys. Rev. Lett. **78**, 1110–1113 (1997).
[27]M. C. Löbl, C. Spinnler, A. Javadi, L. Zhai, G. N. Nguyen, J. Ritzmann, L. Midolo, P. Lodahl, A. D. Wieck, A. Ludwig, and R. J. Warburton, "Radiative Auger process in the single-photon limit," Nat. Nanotechnol. **15**, 558–562 (2020).
[28]M. Geller, "Nonequilibrium carrier dynamics in self-assembled quantum dots," Appl. Phys. Rev. **6**, 031306 (2019).
[29]A. Beckel, A. Kurzmann, M. Geller, A. Ludwig, A. D. Wieck, J. König, and A. Lorke, "Asymmetry of charge relaxation times in quantum dots: The influence of degeneracy," Europhys. Lett. **106**, 47002 (2014).
[30]P. Lochner, A. Kurzmann, J. Kerski, P. Stegmann, J. König, A. D. Wieck, A. Ludwig, A. Lorke, and M. Geller, "Real-time detection of single Auger recombination events in a self-assembled quantum dot," Nano Lett. **20**, 1631–1636 (2020).
[31]A. Kurzmann, A. Ludwig, A. D. Wieck, A. Lorke, and M. Geller, "Auger recombination in self-assembled quantum dots: Quenching and broadening of the charged exciton transition," Nano Lett. **16**, 3367–3372 (2016).
[32]C.-Y. Lu, Y. Zhao, A. N. Vamivakas, C. Matthiesen, S. Fält, A. Badolato, and M. Atatüre, "Direct measurement of spin dynamics in InAs/GaAs quantum dots using time-resolved resonance fluorescence," Phys. Rev. B **81**, 035332 (2010).
[33]M. Kroutvar, Y. Ducommun, D. Heiss, M. Bichler, D. Schuh, G. Abstreiter, and J. J. Finley, "Optically programmable electron spin memory using semiconductor quantum dots," Nature **432**, 81–84 (2004).
[34]J. Dreiser, M. Atatüre, C. Galland, T. Müller, A. Badolato, and A. Imamoglu, "Optical investigations of quantum dot spin dynamics as a function of external electric and magnetic fields," Phys. Rev. B **77**, 075317 (2008).
[35]Z. Wasilewski, S. Fafard, and J. McCaffrey, "Size and shape engineering of vertically stacked self-assembled quantum dots," J. Cryst. Growth **201-202**, 1131–1135 (1999).
[36]A. Ludwig, J. H. Prechtel, A. V. Kuhlmann, J. Houel, S. R. Valentin, R. J. Warburton, and A. D. Wieck, "Ultra-low charge and spin noise in self-assembled quantum dots," J. Cryst. Growth **477**, 193–196 (2017).
[37]A. Högele, S. Seidl, M. Kroner, K. Karrai, R. J. Warburton, B. D. Gerardot, and P. M. Petroff, "Voltage-controlled optics of a quantum dot," Phys. Rev. Lett. **93**, 217401 (2004).
[38]S.-S. Li and J.-B. Xia, "Quantum-confined stark effects of InAs/GaAs self-assembled quantum dot," J. Appl. Phys. **88**, 7171–7174 (2000).
[39]S. T. Yılmaz, P. Fallahi, and A. Imamoğlu, "Quantum-dot-spin single-photon interface," Phys. Rev. Lett. **105**, 033601 (2010).
[40]P. Lochner, J. Kerski, A. Kurzmann, A. D. Wieck, A. Ludwig, M. Geller, and A. Lorke, "Internal photoeffect from a single quantum emitter," Phys. Rev. B **103**, 075426 (2021).
[41]P. Zeeman, "The effect of magnetisation on the nature of light emitted by a substance," Nature **55**, 347 (1897).
[42]M. Kroner, K. M. Weiss, B. Biedermann, S. Seidl, A. W. Holleitner, A. Badolato, P. M. Petroff, P. Öhberg, R. J. Warburton, and K. Karrai, "Resonant two-color high-resolution spectroscopy of a negatively charged exciton in a self-assembled quantum dot," Phys. Rev. B **78**, 075429 (2008).
[43]G. Fernandez, T. Volz, R. Desbuquois, A. Badolato, and A. Imamoglu, "Optically tunable spontaneous Raman fluorescence from a single self-assembled InGaAs quantum dot," Phys. Rev. Lett. **103**, 087406 (2009).
[44]R. J. Warburton, "Single spins in self-assembled quantum dots," Nat. Mater. **12**, 483–493 (2013).
[45]J. Debus, V. F. Sapega, D. Dunker, D. R. Yakovlev, D. Reuter, A. D. Wieck, and M. Bayer, "Spin-flip Raman scattering of the resident electron in singly charged (In,Ga)As/GaAs quantum dot ensembles," Phys. Rev. B **90**, 235404 (2014).
[46]A. V. Khaetskii, D. Loss, and L. Glazman, "Electron spin decoherence in quantum dots due to interaction with nuclei," Phys. Rev. Lett. **88**, 186802 (2002).
[47]B. Urbaszek, X. Marie, T. Amand, O. Krebs, P. Voisin, P. Maletinsky, A. Högele, and A. Imamoglu, "Nuclear spin physics in quantum dots: An optical investigation," Rev. Mod. Phys. **85**, 79–133 (2013).
[48]A. V. Kuhlmann, J. Houel, A. Ludwig, L. Greuter, D. Reuter, A. D. Wieck, M. Poggio, and R. J. Warburton, "Charge noise and spin noise in a semiconductor quantum device," Nat. Phys. **9**, 570–575 (2013).
[49]G. A. Narvaez, G. Bester, and A. Zunger, "Excitons, biexcitons, and trions in self-assembled (In,Ga)AsGaAs quantum dots: Recombination energies, polarization, and radiative lifetimes versus dot height," Phys. Rev. B **72**, 245318 (2005).
[50]A. Kurzmann, B. Merkel, P. Labud, A. Ludwig, A. Wieck, A. Lorke, and M. Geller, "Optical blocking of electron tunneling into a single self-assembled quantum dot," Phys. Rev. Lett. **117**, 017401 (2016).